Supplementary Materials

Supplementary figures

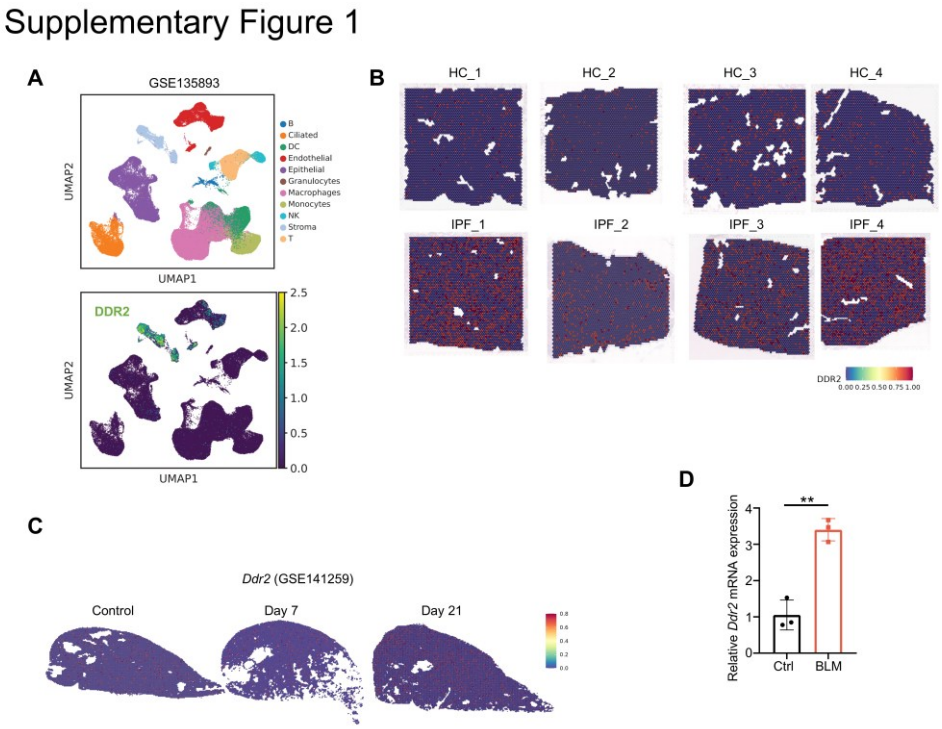

Supplementary figure 1 DDR2 is a stromal biomarker upregulated in PF. (**A**) Analysis of *DDR2* expression in lungs from IPF patients, referring to public scRNA-seq data GSE135893. (**B**) Spatial transcriptomics analysis of DDR2 in lung tissues from healthy donors and patients with IPF from BioStudies data set S-BSST1410. (**C**) Analysis of spatiotemporal *Ddr2* expression in the BLM-instilled mouse lungs, referring to the spatial RNA-seq results from dataset GSE141259. (**D**) RT-qPCR analysis of relative *Ddr2* mRNA levels in the left lungs between healthy and UPF mice (n=3). Data are presented as mean ± SEM. Statistical significance was determined by two-tailed unpaired *Student's t*-test.

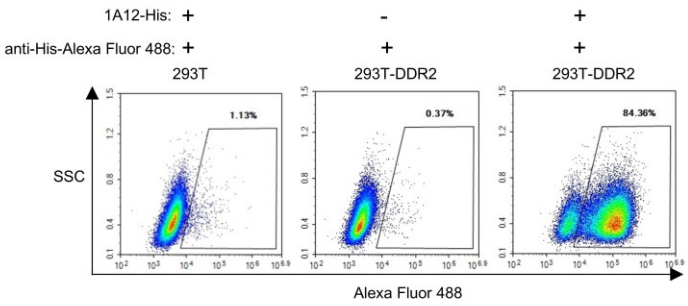

Supplementary figure 2 Nanobody 1A12 binds to surface DDR2. Flow cytometry results showing that nanobody 1A12 specifically bound to 293T-DDR2 cells, but not wild-type 293T cells.

Supplementary Figure 3

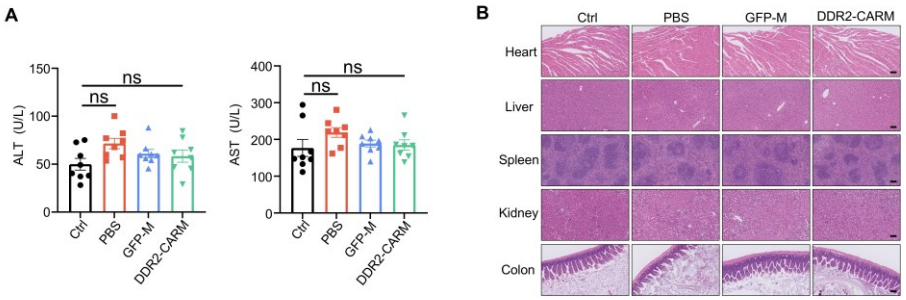

Supplementary figure 3 DDR2-CARM showed no signs of toxicity in mice. (**A**) Serum concentrations of alanine aminotransferase (ALT) and aspartate aminotransferase (AST) in Ctrl mice and UPF mice treated with PBS, GFP-M, or DDR2-CARM as determined by ELISA. (**B**) HE staining of tissue sections of heart, liver, spleen, kidney, and colon from Ctrl mice and UPF mice treated with PBS, GFP-M, or DDR2-CARM. Scale bar, 100 μm.

Supplementary Figure 4

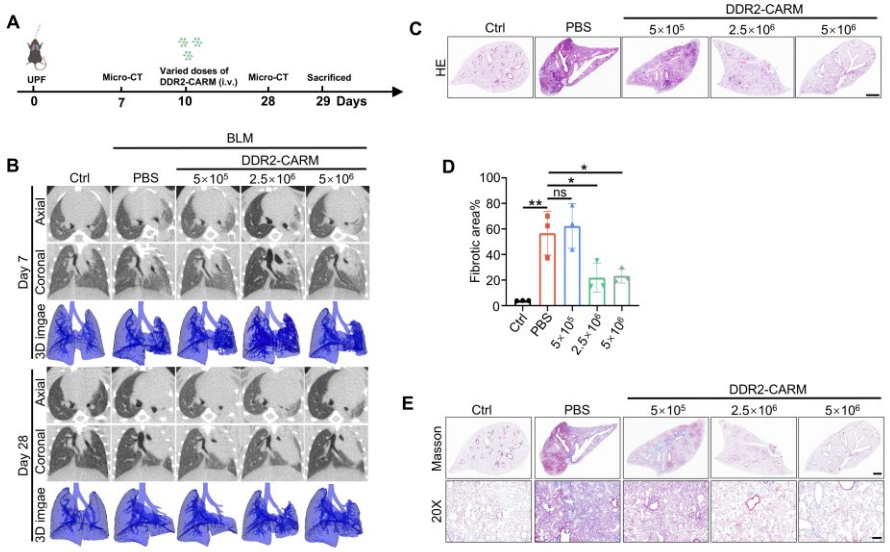

Supplementary figure 4 Dose dependence of the anti-fibrotic efficacy of DDR2-CARM. (**A**) Schematic illustration of the experimental procedures. Different doses of DDR2-CARM were infused on day 10 post BLM instillation. (**B**) Micro-CT images and 3D reconstructions of the lungs from Ctrl mice and UPF mice before (day 7) or after (on day 28) treatment with PBS or varied doses (5×10^5, 2.5×10^6, or 5×10^6 per mouse) of GFP-M or DDR2-CARM. (**C**) Comparison of HE stained sections of the left lungs between different groups of mice. Scale bar, 1 mm. (**D**) Comparison of the fibrotic area percentages within the left lungs from different groups of mice. (**E**) Comparison of Masson's trichome staining of left lung sections from different groups of mice. Upper scale bar, 1 mm. Lower scale bar, 100 μm. Data represent mean ± SD and statistical differences were determined by one-way ANOVA with Tukey's correction. * $p < 0.05$; ** $p < 0.01$; *** $p < 0.001$.

Supplementary Figure 5

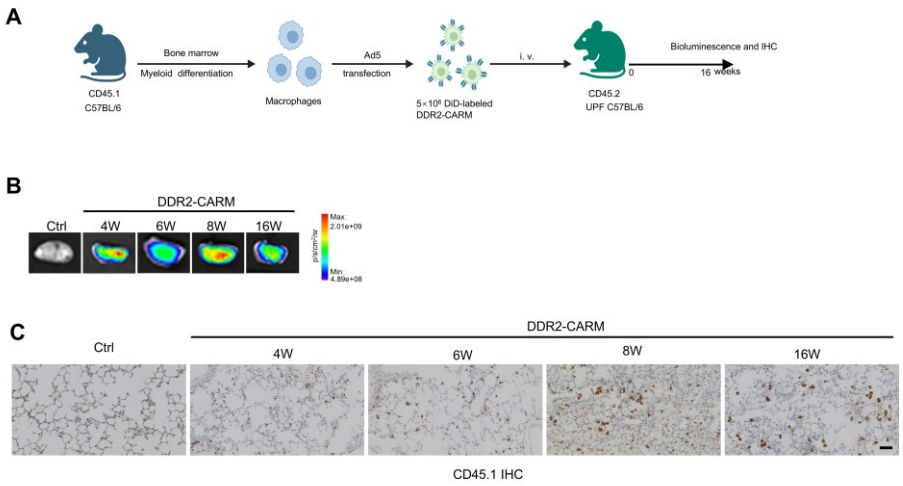

Supplementary figure 5 DDR2-CARM showed long-term persistence as interstitial macrophages in the fibrotic lungs of UPF mice. (**A**) Schematic illustration of longitudinal assessment of DDR2-CARM presence in the fibrotic lungs of UPF mice. (**B and C**) Detection of DiD fluorescence (B) and immunohistochemical staining of CD45.1 (C) in the fibrotic left lungs from Ctrl mice and UPF mice at week 4, 6, 8, and 16 following intravenous infusion of DiD-labeled DDR2-CARM. Scale bar, 100 μm.

Supplementary Figure 6

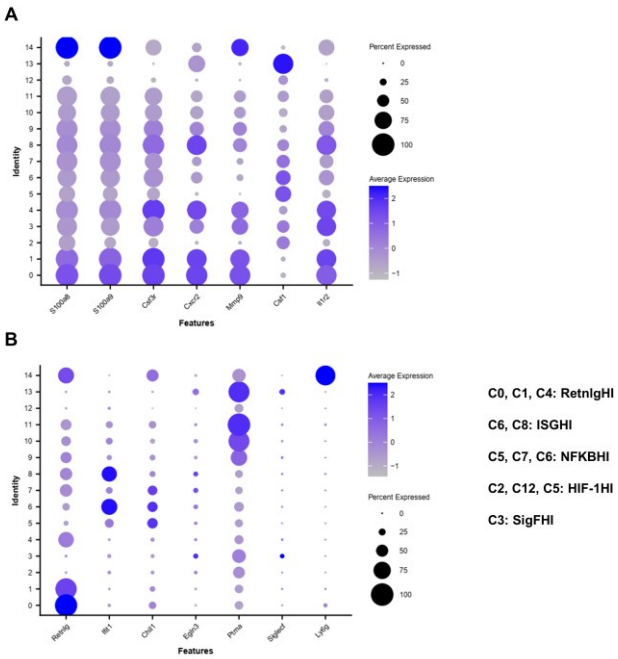

Supplementary figure 6 Sub-clustering of neutrophils from the fibrotic lungs of UPF mice. (**A**) Marker genes used to identify and sub-cluster neutrophils in the fibrotic left lungs of UPF mice. (**B**) 14 clusters of neutrophils were functionally sub-grouped: C0, C1 and C4 were Retnlg^{HI}; C6 and C8 were ISG^{HI}; C5, C7 and C6 were NFκB^{HI}; C2, C12 and C5 were HIF-1^{HI}; and C3 was SigF^{HI}.

Supplementary video 1 Two-photo microscopic analysis of the colocalization of DDR2^{+} stromal cells and GFP-M within BLM-induced fibrotic lung tissues. DDR2-CARM expressed GFP. DDR2^{+} stromal cells were stained with 1A12-Cy3 (red).

Supplementary video 2 Two-photo microscopic analysis of the colocalization of DDR2^{+} stromal cells and DDR2-CARM within BLM-induced fibrotic lung tissues. GFP-M expressed GFP. DDR2^{+} stromal cells were stained with 1A12-Cy3 (red).

Supplementary table 1

	UTD	GFP-M	DDR2-CARM
Estimated Number of Cells	10,214	8,963	9,099
Mean Reads per Cell	30,752	34,575	33,305
Median Genes per Cell	1,752	1,772	1,894
Number of Reads	314,102,724	309,896,951	303,038,188
Valid Barcodes	93.80%	94.50%	93.00%
Sequencing Saturation	64.30%	60.10%	65.90%
Q30 Bases in Barcode	96.80%	97.00%	96.80%
Q30 Bases in RNA Read	92.90%	92.90%	93.10%
Q30 Bases in UMI	97.30%	97.30%	97.30%
Reads Mapped to Genome	89.10%	88.90%	89.00%
Reads Mapped Confidently to Genome	86.00%	85.70%	85.90%
Reads Mapped Confidently to Intergenic Regions	6.70%	6.50%	7.40%
Reads Mapped Confidently to Intronic Regions	13.20%	11.60%	12.00%
Reads Mapped Confidently to Exonic Regions	66.10%	67.60%	66.50%
Reads Mapped Confidently to Transcriptome	74.20%	73.30%	73.90%
Reads Mapped Antisense to Gene	4.90%	5.70%	4.40%
Fraction Reads in Cells	89.90%	63.60%	88.00%
Total Genes Detected	23,506	23,553	23,765
Median UMI Counts per Cell	4,395	4,081	4,651
Number of cells after filtering nFeature_RNA > 400 & nFeature_RNA < 7000 & percent.mt < 15)	9871	8797	8497